Stony Brook University

Stony Brook University

Palmitoylation of the NMDA receptor and PSD95 utilizing Phosphopantetheinyl Transferases

A Thesis Presented

by

Victor Chang

to

The Graduate School

in Partial Fulfillment of the

Requirements

for the Degree of

Master of Science

in

Biochemistry and Cell Biology

Stony Brook University

December 2016

Stony Brook University

The Graduate School

Victor Chang

We, the thesis committee for the above candidate for the

Master of Science degree, hereby recommend

acceptance of this thesis.

Mark E. Bowen– Thesis Advisor
Associate Professor, Department of Physiology and Biophysics

W. Todd Miller – Second Reader
Professor, Department of Physiology and Biophysics

This thesis is accepted by the Graduate School

Charles Taber
Dean of the Graduate School

Abstract of the Thesis

Palmitoylation of the NMDA receptor and PSD95 utilizing Phosphopantetheinyl Transferases

by

Victor Chang

Master of Science

in

Biochemistry and Cell Biology

Stony Brook University

2016

Signal transduction relies on the proper localization of proteins to properly transfer signals throughout the cell. The cell membrane serves as a vital interface for the proper localization of proteins. Posttranslational modifications cause proteins to become targeted to membranes. One such modification is palmitoylation, the addition of a palmitic acid to a cysteine of a protein. Within the neuron, a large protein complex called the postsynaptic density receives upstream signals at the synapse. Many signaling proteins within the postsynaptic density are known to require palmitoylation for proper trafficking and function. Two such examples are the N-methyl-D-Aspartate receptor (NMDAR) and Post Synaptic Density Protein 95 (PSD95). While studies have been carried out on their soluble forms, their palmitoylated forms have not been well studied. This is due to the difficulty in palmitoylating proteins in-vitro. We circumvent this issue by utilizing phosphopantetheinyl transferases (PPTases) to palmitoyate proteins. PPTases are able to attach various Coenzyme A substrates to proteins with specific tag sequences. We also develop a 2-step assay to quantify the effectiveness of the palmitoylation reaction. We successfully show that palmitoylation using AcpS, a PPTase, is possible utilizing the developed assays.

Table of Contents

List of Figures/Tables

List of Abbreviations

Abbreviation	Meaning
A1	12 amino acid peptide sequence that is preferentially targeted by AcpS for attachment of a coenzyme A substrate.
AcpS	A phosphopantetheinyl transferase, 2 types of AcpS used from *E. coli* and *S. pneumoniae*, labels A1 and Y1 tag
CoA	Coenzyme A, substrate for phosphopantetheinyl transferase, Ppant arm is attached to protein.
DHHC	Aspartate- Histidine-Histidine-Cysteine, a family of proteins containing the conserved stated residues. PATs are members of the DHHC family of proteins.
DTT	Dithiothreitol
EDTA	Ethylenediaminetetraacetic acid
GluN2B	Subunit of the NMDA receptor
Ni-NTA	Nickel - Nitrilotriacetic acid, captures proteins with a 6x Histidine tag
NMDAR	N-methyl D-Aspartate Receptor, glutamate ion-channel receptor in the post-synapse. Abbreviation after the – represents the tag attached to the particular NMDA protein
Palmitoylation	The posttranslational attachment of a palmitatic acid to a protein
PAT	Palmitoyl transferases, enzymes that are responsible for catalyzing the attachment of palmitate to proteins
PIC	Protease inhibitor cocktail I
PMSF	Phenylmethanesulfonyl fluoride, protease inhibitor
PPT	Phosphopantetheine, moiety that is attached to CoA, contains substrate that will be attached to the protein by PPTase
PPTase	Phosphopantetheinyl transferase, enzyme that attaches a CoA-substrate to a serine in a peptide tag sequence.
PSD	Post synaptic density, large complex of proteins located in the post-synapse
PSD95	Post synaptic density protein 95, Scaffolding protein in post synaptic density, interacts with NMDA receptor, abbreviation after the – represents the tag attached to the particular PSD95 protein.
S6	12 amino acid peptide sequence that is preferentially targeted by Sfp for attachment of a coenzyme A substrate.
Sfp	A phosphopantetheinyl transferase, labels S6 and Y1 tag
TCEP	tris(2-carboxyethyl)phosphine
Ybbr (Y1)	11 amino acid peptide sequence that is targeted by AcpS and Sfp for attachment of a coenzyme A substrate.
βME	β-mercaptoethanol
BOG	N-octyl-β-D-glucoside

Acknowledgments

I would like to thank Fang Wu for help in the expression and purification of many of the constructs used in this thesis. I would like to thanks Brie Levesque, Frank Mindlin, and Zhuojun Guo for their guidance in the lab.

Finally, I would like to thank Mark Bowen, for his guidance and advice that extended well beyond the walls of the lab.

Introduction

Signal transduction pathways are the cascade of signaling molecules and proteins that serve as the cell's method of sensing stimuli. They allow the cell to receive information on their surroundings to formulate a response. One roadblock in signal transduction is transmitting an exterior signal into the cell. The cell membrane blocks most signaling molecules, so signal pathways must often start at the cell membrane. Membrane receptors serve as the main method to receive outside stimuli, which activate downstream pathways (Berg et al. 2002). The cell membrane serves as a critical interface for receptors and signaling proteins to facilitate the pathway interactions necessary for downstream pathway initiation.

Proper localization is required for signal pathway activation. Membrane targeting is used to traffic proteins intracellularly, either to important signaling areas such as the cell membrane, or areas of sequestration (Bhattacharya et al. 1995). Also, by tethering proteins to the cell surface, membrane targeting increases the probability of proteins accessing interaction targets that are located at the cell surface, such as receptors. Besides just location, tethering can also lead to structural changes that increase signaling, such as causing changes in ligand specificity (Xue et al. 2004). Membrane targeting has been shown to serve a critical role for signaling function in various pathways.

One method of membrane targeting is the attachment of a long lipophilic group, such as a fatty acid, to a protein (Folch et al. 1951). This modification leads to an increase in hydrophobicity and the subsequent attachment of the protein to the lipid membrane (Resh

et al. 2006). One lipid-modification that has been discovered is S-palmitoylation. S-palmitoylation is the reversible attachment of a saturated 16-carbon palmitic acid to the protein via cysteine residues on diverse tag sequences. Palmitoylation is mediated by palmitoyl-transferases (PAT) that are members of the conserved DHHC (aspartate–histidine–histidine–cysteine) residue containing family (Roth et al. 2002). S-palmitoylation is distinct from other lipid modifications in being reversible, unlike N-myristoylation and farnesylation (Resh et al. 2006).

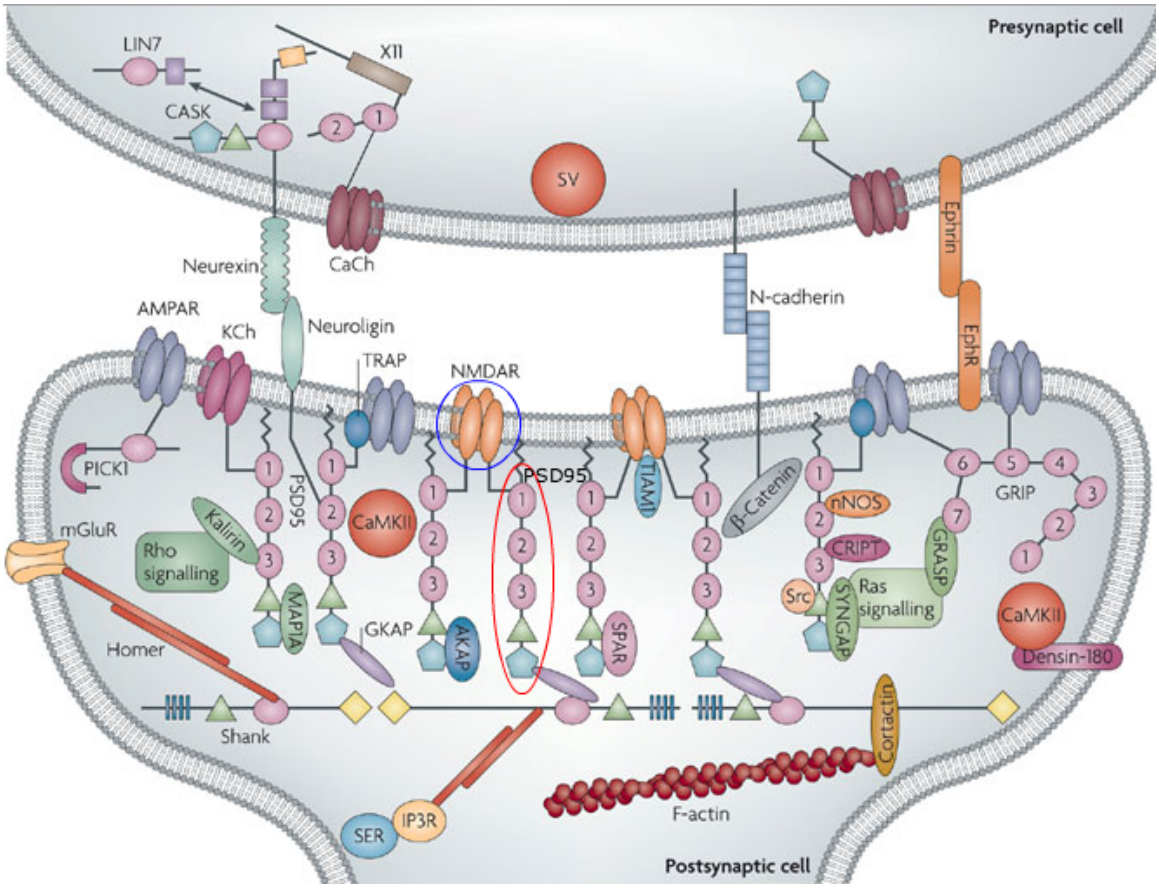

Figure 1 - Structure of the postsynaptic density. The postsynaptic density is a large complex of proteins located in the cell that receives the upstream signals. The N-methyl D-aspartate receptor is circled in blue and PSD95 is circled in red. (Taken from Neff et al. 2009)

Palmitoylation is known to be particularly important in the synapse for proper neuron function and development (el-Hussenini et al. 2000). The synapse serves as the

primary location of signal transduction, ensuring proper communication between neurons. The synapse is composed of the 2 cells; the pre-synaptic cell that sends the signal and postsynaptic cell that receives the signal (Scannevin et al. 2000). A large network of proteins, called the postsynaptic density (PSD) receives the signals sent by the pre-synapse (figure 1) (Feng et al. 2009). In order to localize the signaling molecules and receptors required to form a functioning PSD, synaptic proteins are targeted to the post-synapse by palmitoylation (el-Hussenini et al. 2000). Two proteins that are commonly found palmitoylated in the postsynaptic density are the N-methyl-D-Aspartate receptor (NMDAR) and PSD95 (post synaptic density protein 95).

The NMDAR is a glutamate receptor. Glutamate receptors serve as vital targets for the majority of excitatory neurotransmissions from the presynaptic neuron. The NMDAR is of particular interest due to its unique role in long-term potentiation and synaptic plasticity (Paoletti et al. 2013). This allows NMDAR to have lasting effects on a synapse's form and function. Palmitoylation has shown to be necessary for proper NMDAR trafficking. NMDAR surface expression is regulated by palmitoylation of the cysteine clusters within the GluN2A or GluN2B subunit (Hayashi et al. 2009). Palmitoylation of the 1st cysteine cluster near the membrane-spanning region increases tyrosine phosphorylation of tyrosine-based internalization motifs by Src protein kinases, which leads to increased surface expression of NMDARs in the PSD. If the 2nd cysteine cluster in the C-terminus is palmitoylated, NMDARs instead concentrate in the golgi apparatus (Hayashi et al. 2009).

PSD95 is a key scaffolding protein of the MaGUK family in the PSD, serving as a link between NMDARs and other important proteins in the PSD (Sheng 2001). Scaffolding

proteins tether proteins to help localize interacting partners together. PSD95 is made up of 3 PDZ domains, 1 GuK domain and 1 SH3 domain. The PDZ1-PDZ2 domains bind to C-terminal motifs present in the NMDA receptor GluN2 subunit. PSD95 is known to gather NMDA receptors into clusters within the postsynapse, which would play a large role in signal sensitivity of the dendritic spine (Sheng et al. 2001). Palmitoylation has been shown to be essential for PSD95 function. PSD95 requires palmitoylation of both cysteine sites in order to be correctly sorted from the ER to the postsynapse (El-Husseini et al. 2000). This was shown by mutating the 2 cysteines in the N-terminus to serines, preventing palmitoylation of PSD95. Without palmitoylation, PSD95 cannot be targeted to the PSD and is instead found diffuse throughout the cytoplasm. Consequently, PSD95 cannot cause ion channel clustering, which severely impacts synaptic strength (El-Husseini et al. 2002). Palmitoylation has also been shown to serve as a method of regulating PSD95, due to S-palmitoylation's reversibility. When nitrous oxide, NO, is produced by nNOS, a binding partner for PSD95, S-nitrosylation may occur to PSD95 at the Cys3 and Cys5 locations of the N-terminus. By directly competing with palmitoylation, NO production results in a negative feedback loop leading to the down-regulation of PSD95 clustering in the postsynapse (Ho et al. 2011).

However, despite the heavy research that has been done on the *in vivo* effects of palmitoylation on the NMDAR and PSD-95, the specific effects palmitoylation has on NMDAR and PSD-95 are unknown (Fukata et al. 2004). Coupled with the ability of palmitate to naturally detach from the protein, these complications has resulted in a lack of *in vitro* studies on palmitoylated NMDAR and PSD-95, with most studies focused on their soluble forms instead. It is therefore important to study their natively palmitoylated forms

in the synapse to determine possible structural or kinetic differences with their soluble forms.

While there have been studies on the structure and binding kinetics of PSD-95 in their soluble form, palmitoylation may result in drastic changes of protein dynamics (Zhang et al. 2013) (Chi et al. 2010). It is already been shown that palmitoylation can result in structural changes of the tethered protein, resulting in changes in ligand specificity (Xue et al. 2004). Tethering a protein to the lipid bilayer has also been predicted to cause large changes in diffusional rate and binding kinetics. Membrane tethering via palmitoylation would cause the protein to be limited to lipid-like 2-dimensional diffusion along the bilayer, compared to 3-dimensional diffusion in the cytosol. This reduction in dimensionality would theoretically increase the ability of the tethered protein to find binding partners located on or close to the surface (Berg et al. 1985). We wish to more closely study the palmitoylated forms of NMDAR and PSD95 in-vitro utilizing single molecule fluorescence methods.

In order to study the effects of palmitoylation on structure and binding kinetics, we circumvent the issues of protein palmitoylation using PATs by utilizing an alternative acyl transferase, phosphopantetheinyl transferases (PPTase). PPTases are enzymes that attach the phosphopantetheine (PPT) arm of a coenzyme A molecule (CoA) and attach it to a serine within a peptide tag, with the help of a Mg^{2+} cofactor (Lambalot et al. 1996). PPTases are commonly found in both prokaryotes and eukaryotes, with the ability to attach various substrates. Two commonly used PPTases for lab studies are Sfp and AcpS, each with their own specificity for specific tag sequences (Zhou et al. 2007). Sfp are AcpS are acyl-carrier proteins that can attach lipids of varying length to proteins. Unlike S-palmitoylation, this

reaction is non-reversible, allowing for a stable palmitoylated form to study. This project deals with the issues that arise using PPTases for palmitoylation, and attempts to develop a consistent and effective methodology for palmitoylation using PPTases. We also work towards developing a reliable and cost-effective method to measure the palmitoylation efficiency of various PPTases.

Methods

Expression of protein in E. coli

Constructs containing the sequences for the GluN2B C-terminus and full length PSD95 with the PPTase tags were inserted into the pPROEX HTB vector (Invitrogen, Carlsbad, CA). Three tags for PPTases were used: the A1, S6, and Ybbr (Y1) tag (Zhou et al 2007). A 6-Histidine tag was also added in the N-terminus of all proteins to allow for affinity purification by ni-NTA beads. All constructs were transformed into competent BL21(DE) *E. coli* cells. Colonies were then chosen and a preparatory culture was grown overnight in kanamycin or ampicillin. The culture was then allowed to grow in 1 liter of terrific broth in the presence of kanamycin or ampicillin at 37° C until an OD of 0.6 was reached. Expression was then induced with 1 mM IPTG at 30° C for 2 hours. The cells were then spun down and frozen with liquid nitrogen for storage at -80° C.

Expression of B. subtilis Sfp in E. coli

The *B. subtilis Sfp* plasmid used was a gracious gift from Dr. James B. Munro labs (Munro et al. 2014). The Sfp was received in a pET29 plasmid vector originally described by (Yin et al. 2006). A preparatory culture was grown overnight in the presence of kanamycin. The culture was then grown in the presence of kanamycin at 37° C in 1 liter of terrific broth until an OD of 0.6 was reached. Expression was then induced with 1 mM IPTG at 30° C for 2 hours. The cells were then spun down and frozen with liquid nitrogen for storage at -80° C.

Expression of AcpS in E. coli

AcpS was utilized from 2 different species, *E. coli* and *S. pneumoniae*. The AcpS from *E. coli* was also a gift from James B. Munro labs (Munro et al. 2014). *E. coli* AcpS was received in a pET29 plasmid vector according to previous protocols described by (Yin et al. 2006). A preparatory culture was grown overnight in the presence of kanamycin. The culture was then grown in the presence of kanamycin at 37° C in terrific broth until an OD of .6 was reached. Expression was then induced with 1 mM IPTG at 30° C for 2 hours. The cells were then spun down at and frozen with liquid nitrogen for storage at -80° C.

S. pneumoniae AcpS in a pET15b vector was purchased from Addgene (Plasmid #63687). The AcpS was grown overnight in the presence of ampicillin. The cells were then grown in the presence of ampicillin at 37° C in terrific broth until an OD of .6 was reached. Expression was then induced with 1 mM IPTG at 30° C for 2 hours. The cells were then spun down and frozen with liquid nitrogen for storage at -80° C.

Protein Purification of PSD95

The cell pellet was resuspended in a buffer of 50 mM phosphate, 300 mM NaCl and 1 mM β-mercaptoethanol (βME), pH 7.4. To prevent degradation of the protein, 10 µL/mL of Phenylmethanesulfonyl fluoride (PMSF) and 1 µL/mL of protease inhibitor cocktail I (PIC I) were added to the bacteria suspension before and during lysis via sonication. The PIC consisted of a combination of Antipain, Leupeptin, Benamidine, and BPT1 (bovine pancreatic trypsin inhibitor). The cells were then lyzed as above. The cell lysis was then centrifuged to remove cellular debris. The supernatant containing the soluble proteins was

then incubated in a column with 3 mL bed volume of Ni-NTA beads for 1 hour at 4° C. The column was then drained and the flowthrough was collected. After washing the Ni-NTA beads with the lysis buffer, the protein was then eluted from the nickel beads with 50 mM phosphate, 300 mM NaCl and 250 mM imidazole with 1 mM βME, pH 7.4. The pooled elutions were then dialyzed overnight in aHEPES-buffered saline solution of 25 mM HEPES, 200 mM NaCl with 1 mM dithiothreitol (DTT), and 1 mM Ethylenediaminetetraacetic acid (EDTA). Further purification was then done using gel filtration utilizing a Sephadex 200 column and FPLC.

Protein Purification of NMDAR GluN2B C-terminus

The cell pellet was resuspended in 100 mM phosphate, 10 mM Tris, 300 mM NaCl, 1 mM βME, and 8 M urea, pH 8. To prevent degradation of the protein, 10 µL/mL of PMSF and 1 µL/mL of PIC I were added to the bacteria suspension before and during lysis via sonication. The cells were then lyzed as above. The cell lysis was then centrifuged to remove cellular debris. The supernatant containing the soluble proteins was then incubated in a column with a 3 mL bed volume of Ni-NTA beads for 1 hour at room temperature. The column was then drained and the flowthrough was collected. After washing the Ni-NTA beads with the lysis buffer, the protein was eluted from the nickel beads with 50 mM phosphate, 300 mM NaCl, 2 M urea and 250 mM imidazole, 1 mM βME, pH 8. The pooled elutions were then dialyzed overnight in Tris-buffered saline with 20 mM Tris, 50 mM NaCl, 2 M urea, 1 mM DTT, and 1 mM EDTA. TEV protease was added after dialysis to remove the 6-Histidine tag. Further purification was then done using cation exchange chromatography in 20 mM MES, 0-1 M NaCl, 2 M urea, and 0.5 mM DTT, pH 6.0.

Protein Purification for Sfp

Sfp was purified according to the protocol from (Yin et al. 2006) with some modifications. The bacteria suspension was resuspended in 20 mM Tris, 500 mM NaCl, 5 mM Imidazole, 10 mM $MgCl_2$, 1 mM βME, pH 7.9. To prevent degradation, 10 µL/mL of PMSF and 1 µL/mL of PIC I. 2 units/mL of DNase was added as well to reduce DNA nonspecific binding. The cells were lysed via sonication instead of French pressure cell press. The cells were then lyzed as above. The cell lysis was then centrifuged to remove cellular debris. The supernatant containing the soluble proteins was then incubated in a column with 2 mL bed volume of Ni-NTA beads for 1 hour at 4° C. The column was then drained and the flowthrough was collected. After washing the Ni-NTA beads with the lysis buffer, the protein was then eluted from the nickel beads with 20 mM Tris, 500 mM NaCl, 250 mM imidazole and 1 mM βME, pH 7.9. The pooled elutions were then dialyzed overnight in 10 mM Tris, 1 mM DTT, 1 mM EDTA and 10% glycerol.

Protein Purification for E. coli AcpS

Two lysis buffers were attempted, a denaturing buffer containing urea and a buffer containing no urea. The denaturing lysis buffer was 20 mM Tris, 2 M urea, 10 mM $MgCl_2$, 10 mM Imidazole, .5 mM βME, pH 8. The cell pellet was resuspended in the lysis buffer. 10 µL/mL PMSF and 1 µL/mL PIC I were added to the bacteria suspension before and during lysis via sonication. The cells were then lyzed as above. The cell lysis was then centrifuged to remove cellular debris. The supernatant containing the soluble proteins was then incubated in a column with 4 mL bed volume of Ni-NTA beads for 1 hour at room temperature. The column was then drained and the flowthrough was collected. The protein

was then eluted from the nickel beads in Tris-buffered saline of 50 mM Tris, 300 mM NaCl, 250 mM imidazole, and 1 mM βME. The elutions were immediately diluted 3-10 times, until precipitation was noted to stop occurring. The elutions were centrifuged and the supernatant was then dialyzed overnight in several different buffers (see *Results*).

Protein Purification for S. pneumoniae AcpS

Two lysis buffers were attempted, a denaturing buffer containing urea and a buffer containing no urea. The denaturing lysis buffer was first attempted with 20 mM Tris, 2 M urea, 10 mM $MgCl_2$, 10 mM Imidazole, .5 mM βME, pH 8. A second lysis was attempted with 50 mM phosphate, 300 mM NaCl, and 1 mM βME, pH 7.4. 10 µL/mL PMSF and 1 µL/mL PIC I were added to the bacteria suspension before and during lysis via sonication. The cells were then lyzed as above. The cell lysis was then centrifuged to remove cellular debris. The supernatant containing the soluble proteins was then incubated in a column with 3 mL bed volume of Ni-NTA beads for 1 hour at 4° C. The column was then allowed to flow through for collection. The protein was then eluted from the nickel beads with 50 mM phosphate, 300 mM NaCl, 250 mM imidazole and 1 mM βME, pH 7.4. The elutions were then diluted 3 times. The pooled elutions were then dialyzed overnight in 50 mM phosphate, 300 mM NaCl, 1 mM DTT, and 1 mM EDTA.

Protein Purification Quality and Solubility Test

Samples were collected throughout the purification process for testing. Samples after lysis and after centrifugation were collected, labeled “total” and “soluble” respectively. After protein incubation with the Ni-NTA beads, the flow through of the binding column

that contained the unbound proteins was also collected and labeled “flowthru”. These samples, along with samples of the elution fractions, were run on a SDS-page gel to determine relative purity and concentration of the desired protein.

Protein labeling with Alexa Dyes

500 µL of the protein was incubated with 5 mM DTT for 1 hour. The protein was then buffer exchanged to a HEPES-buffered saline solution of 25 mM HEPES, and 200 mM NaCl containing 0.5 mM tris(2-carboxyethyl)phosphine (TCEP). This was done with a PD-10 desalting column (GE-Healthcare). 10 nmol of the protein was then reacted overnight with 50 nmol aliquot of dried maleimide Alexa dye, either Alexa 555 or Alexa 647 (Invitrogen, Carlsbad, CA). The protein was then separated from the free Alexa dye with a Sephadex G-50 size exclusion column (GE Healthcare). The labeling efficiency was then measured by measuring the protein absorbance at 280 nm and the dye absorbance at 555 nm or 651 nm.

Coenzyme-A Labeling with PPTases

The protocol used was modified from the Sfp protocols from New England Biolabs, and from (Yin et al. 2006). The labeling reaction was consisted of 20 mM Tris, pH 7.4, 7 mM $MgCl_2$, 1 µM PPTase enzyme (AcpS or Sfp), 5 µM (A6, S6, or Y1) tagged protein, and 20 µM CoA substrate (Palmitate-CoA or Fluorescein-CoA). Detergents were also used in the labeling reaction: 50 mM N-octyl-β-D-glucoside (βOG), 4 mM CHAPS, 0.1%, 0.02% (w/w) Triton X-100, 0.1%, or 0.01% (w/w) Tween 20. This was to aid in palmitate-CoA solubility. The reaction was then incubated at room temperature for 1 hour or at 4° C overnight.

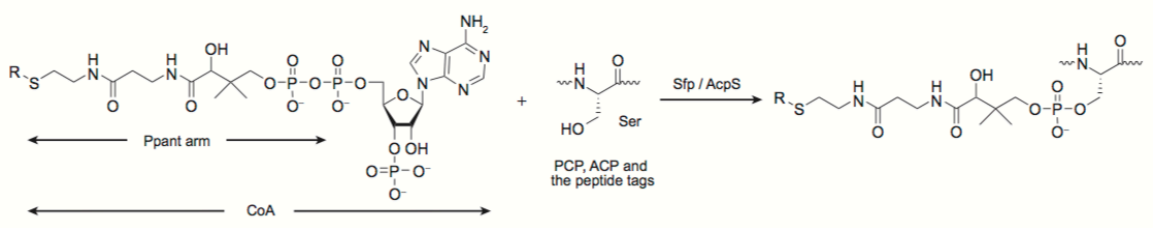

Figure 2 - Attachment of the Phosphopantetheine (PPant) arm of Coenzyme A to a target sequence via PPtases. (Taken from Zhou et al. 2007) The CoA molecule, which contains the Ppant arm with the substrate of interest, is reacted to a serine by the PPTase (Sfp or AcpS).

Fluorescein Chase Experiment

A first labeling reaction with palmitate-CoA was carried out with the protein according to the Coenzyme-A method above. After 1 hour or overnight, fluorescein-CoA was added to a final concentration of 20 μM for a second labeling reaction with fluorescein-CoA. The fluorescence was then determined by SDS-page.

Detecting Liposome-Bound Fluorescently Labeled Proteins

Alexa labeled protein was tagged with palmitate-CoA according to the protocol above. 50 nm diameter liposomes composed of Egg phosphatidylcholine (Avanti Lipids, Alabaster, AL) were extruded according to the protocol by (Choi et al. 2012). The palmitoylated protein was then incubated with the liposomes for 10 minutes to allow for the protein to attach to the liposome. The liposomes were then separated from the unbound protein by a size exclusion chromatography using a Sepharose CL-4B column (GE Healthcare) with elutions collected every 200 μL. A sample of control liposomes was also separated by size exclusion chromatography to serve as a reference sample. This was required due to liposomes exhibiting fluorescence due to Rayleigh scattering effects. The fluorescence of the elutions containing the separated liposomes and free protein were then

measured by a fluorometer to determine the concentration of bound protein to the liposomes.

Results

Preparation and Purification of PPTase Tag Constructs and PPTases

Three tag sequences were used to tag the NMDA receptor and PSD95: the A1 tag, S6 tag and Ybbr(Y1) tag (table 1). The C-terminal tail of the GluN2B subunit of the NMDA receptor was used for study of the NMDA receptor, while the full length PSD95 was used. The peptide tag was added to the N-terminus of the protein sequence, along with a 6-Histidine tag to allow for protein capture with Ni-NTA chromatography. All cysteines in all our proteins, except 1 natural cysteine, were replaced with serines for both the NMDA receptor and PSD-95. This was to allow us to use maleimide dyes to tag the protein for fluorescence studies. Three PPTases were used in conjunction with these tags, *E. coli* AcpS, *B. Subtilis* Sfp and *S. pneumoniae*.

Peptide Tag	Peptide Sequence	PPTase Specificity	Constructed Proteins
A1	GDSLDMLEWSLM	AcpS	NMDA-A1
S6	GDSLSWLLRLLN	Sfp	PSD95-S6
Ybbr	DSLEFIASKLA	AcpS & Sfp	NMDA-Y1, PSD95-Y1

Table 1 – PPTase Tag Constructs. The A1, S6, and Ybbr PPTase peptide tags were utilized from (Zhou et al. 2007). The peptide sequences attached to the N-terminus are shown under "Peptide Sequence". The underlined S shows the serine that is attached with the CoA substrate. The specific PPTase that recognizes the tag is shown under "PPTase Specificity". Finally, the proteins constructed and tested are shown under "Constructed Proteins".

Previous research by Joshua Ha and Omkar Venkatesh showed that tagged constructs of the NMDAR and PSD95 could be successfully expressed in *E. coli* cells. However, difficulties in solubility were found to arise during purification. Despite only a short 11 or 12 peptide chain added to the N-terminus of the protein, the tag was found to have a significant impact on solubility. Both the NMDA receptor GluN2B C-terminus with the A1 tag (NMDA-A1), and PSD95 with the S6 tag (PSD95-S6) were noted to have

precipitation occur during the purification of the protein. For the constructs used, 2 proteins were noted to have large scale issues in purification, NMDA-A1 and AcpS.

NMDA-A1 Solubility Requires Use of Detergents

The previous research by Joshua Ha and Omkar Venkatesh with NMDA-A1 had significant precipitation during elution and dialysis of the protein (figure 3). To reduce the precipitation, the pH and NaCl concentration were modified to optimize NMDA-A1 solubility. NMDA-A1 was desalted using a PD-10 desalting column (GE Healthcare) from the dialysis buffer, 20 mM Tris, 50 mM NaCl, and 2 M Urea, pH 7.4 buffer into phosphate-saline buffers with 50 mM phosphate, with a pH range of 6.2-8, and NaCl concentrations of 50-500 mM (Table 2). The amount of protein was then determined by absorbance at 280 nm. It was determined that a pH of 7-8 and a NaCl concentration of 300-500 were ideal for NMDA-A1 solubility.

pH	NaCl (mM)	Concentration(μM)
6.2	300	9.9
6.2	500	8.3
7	50	7.9
7	300	10.5
7	500	10.7
8	50	5.9
8	300	11.0
8	500	9.1

Table 2- Concentration of NMDA-A1 under various salt and pH conditions. Samples of NMDA-A1 with an initial concentration of 15 μM were dialyzed into solutions containing the pH and NaCl concentrations listed. The best conditions are highlighted in green.

In addition, detergents were also used to further attempt to increase the solubility of NMDA-A1. NMDA-A1 was dialyzed into a 50 mM phosphate, 300 mM NaCl, pH 7.4 buffer with different detergents. The detergents concentrations were set to double their critical micelle concentration (CMC)

Detergent	Detergent Concentration
N-octyl-β-D-glucoside (βOG)	50 mM
Deoxycholic Acid (DOC)	12 mM
Dodecyl Molticide (DDM)	1.2 mM
Thesit	.16 mM

Table 3- Detergents tested to increase solubility of NMDA-A1. Detergent concentrations were chosen to be 2x the CMC. The detergents were in a 50 mM phosphate, 300 mM NaCl, pH 7.4 buffer.

(table 3). After dialysis overnight, the NMDA-A1 samples were collected, and spun down to remove any precipitation. The concentration of NMDA-A1 in the supernatant was then quantified by SDS-page. After staining, we found that DOC resulted in the highest protein concentration of NMDA-A1, followed by βOG (figure 3).

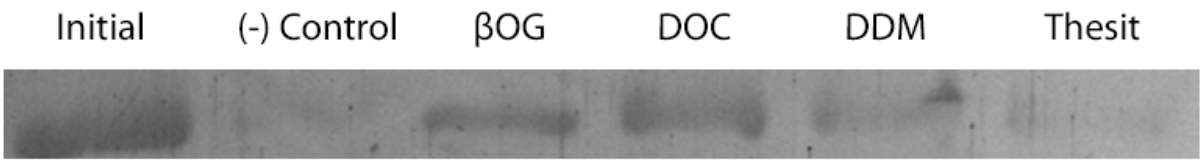

Figure 3 – SDS PAGE gel of dialyses of NMDA-A1. Initial shows the NMDA-A1 band before dialysis, showing the original concentration. (-) Control shows a dialysis with no detergents present, with just a phosphate saline buffer. βOG, DOC, DDM, and Thesit show the bands of NMDA-A1 corresponding to that detergent. DOC, followed by βOG, shows the greatest concentration of NMDA-A1.

E. Coli AcpS shows Limited Solubility

Previous work by Ha and Venkatesh also reported difficulty in successfully producing active AcpS without protein precipitation. While urea was found to keep AcpS soluble, the AcpS proved to be inactive in a urea buffer. Dialysis also proved to be a challenge, due to the tendency of AcpS to completely precipitate at temperatures colder than room temperature.

To reduce precipitation, various dialyses from several sources were attempted. Published papers reported a large variation in *E. coli* AcpS purification protocols. *E. coli* AcpS was lysed in 50 mM Tris, 500 mM NaCl and 5 mM imidizole, 1 mM βME, pH 8 and 1 unit/mL DNase1 and eluted in 50 mM Tris, 300 mM NaCl, 250 mM imidazole, and 1 mM βME. The pooled elutions were then split and dialyzed into various buffers containing different detergents. The buffers were chosen based on published papers on *E. coli* AcpS preparation and purification from several sources: Munro Labs (Munro et al. 2014), (Yin et al. 2006), (Sunbul et al. 2009) and the NEB patent on AcpS (Johnsson et al. 2010) (table 4).

The sample concentrations were then measured by absorbance. The only dialysis buffer that proved acceptable was the Bis-Tris Propane buffer with a concentration of 153 μM, which was stored in -80° C. Results showed that AcpS was most soluble in buffers containing high salt. Both the Bis-Tris Propane buffer and the MES buffer, each containing 500 mM NaCl, performed the best.

Dialysis Buffer	AcpS Concentration
100 mM Bis-Tris Propane, 500 mM NaCl, pH 6	153 μM
10 mM Tris pH 7.5	13 μM
50 mM MES, 500 mM NaCl, pH 6	28 μM
50 mM HEPES, pH 7.2	7 μM

Table 4- Dialysis of *E. coli* AcpS using recommended dialysis buffers. Buffers used are from (Sunbul et al 2009), Yin et al. 2006), (Munro et al. 2014) and (Johnsson et al. 2010) respectively. Bis Tris Propane proved the most efficient at keeping AcpS soluble.

S. Pneumoniae AcpS Shows no Issues with Solubility

S. pneumoniae AcpS was successfully produced in competent *E. coli* cells. The cells were lysed using a phosphate saline buffer containing 50 mM phosphate, 300 mM NaCl, and 1 mM βME, pH 7.4. This was to prevent any precipitation that may have occurred, similar to *E. coli* ApcS. The protein was then dialyzed in Bis-tris propane, MES, MES with urea, and phosphate-saline buffer under native conditions (table 5). These were chosen based on the results with *E. coli* AcpS, with the addition of a native buffer and a urea buffer (table 4). However, we found that *S. pneumoniae* AcpS did not precipitate as expected, instead proving soluble in all conditions. Since the AcpS showed no signs of requiring specific

Dialysis Buffer	AcpS Concentration
100 mM Bis-Tris Propane, 500 mM NaCl pH 6	192 μM
50 mM MES, 500 mM NaCl, pH 6	179 μM
20 mM MES, 2 M Urea, pH 6	153 μM
Native PBS: 50 mM phosphate, 300 mM NaCl, pH 7.4	171 μM

Table 5 – Dialysis of *S. pneumoniae* AcpS, and the resulting concentration. S. pneumonie shows no sign of precipitation in any dialysis. The change in species shows a drastic difference in solubility.

buffers for solubility, a general native elution was used and dialyzed in the native PBS buffer.

Evaluation and Selection of PPTase and PPTase Tag

Mg^{2+} is required for PPTase Activity

Previous research by Ha had difficulty in keeping palmitate-CoA in a soluble, accessible form for the PPTase to utilize. Published data showed that Mg^{2+} concentrations greater then 7 mM had a large effect on the solubility of palmitate-CoA (Constantinides et al. 1985). Thus, we wanted to determine the minimum concentration of Mg^{2+} required for PPTase activity, to reduce palmitate-CoA precipitation. NMDA-A1 was labeled with fluorescein-CoA using *E. coli* AcpS with 2.5, 5, and 7.5 mM Mg^{2+}. The NMDA-A1 was then separated from the free fluorescein-CoA using a PD-10 buffer exchange column. The concentration of NMDA-A1 and the fluorescein was then determined using absorbance spectroscopy to find the tag efficiency, the percentage of NMDA-A1 protein that was actually labeled with fluorescein-CoA. The tag efficiency was noted to be low with all concentrations of Mg^{2+}, less than 25%. A concentration of 7.5 mM was determined to have the greatest tag efficiency and a concentration of 7 mM used, to allow the absolute max Mg^{2+} concentration without precipitation of the palmitate-CoA (table 1).

Concentration Of Mg^{2+}	Tag Efficiency
2.5 mM	0.13
5 mM	0.19
7.5 mM	0.21

Table 6 – Tag efficiency depends on Mg^{2+} Concentration. The fraction of protein that was labeled over the total original protein was used to find the tag efficiency. The higher the Mg^{2+} concentration, the higher the tag efficiency.

Sfp Exhibits Greater Labeling Efficiency than E. coli AcpS with Fluorescein-CoA

NMDA-Y1 (NMDA GluN2B C-terminus with a Ybbr tag) was constructed and purified under denaturing conditions with urea and it was found that NMDA-Y1 did not have the same problems with solubility as NMDA-A1. Since the Ybbr tag can be recognized by both AcpS and Sfp (Zhou et al. 2007), NMDA-Y1 was used to compare the labeling efficiency of *E. coli* AcpS and Sfp. NMDA-Y1 was labeled with fluorescein-CoA using both Sfp and *E. coli* AcpS. The protein was then separated from the free fluorescein-CoA by SDS-page and imaged for fluorescence. Results showed that Sfp had a much higher fluorescence then AcpS, leading to the conclusion that Sfp had a greater fluorescein labeling efficiency then AcpS (figure 4). Sfp activity also showed the ability to label itself in cases of excess fluorescein-CoA. Due to Sfp having greater activity then *E. coli* AcpS, we decided to first focus efforts on Sfp.

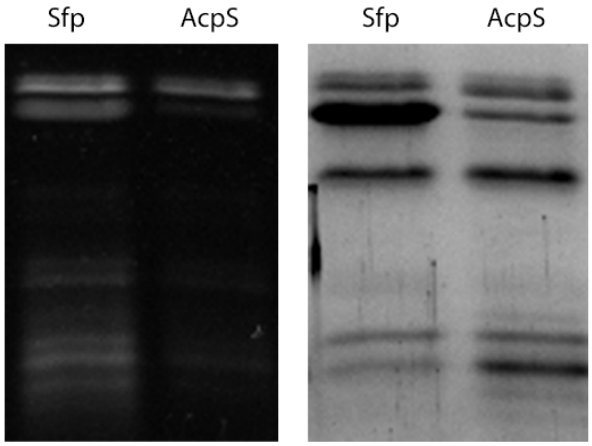

Figure 4 – Fluorescein-CoA Labeling of NMDA-Y1 by Sfp and AcpS. Left, fluorescence image of gel, NMDA-Y1 is the topmost band. Sfp shows much greater fluorescence than AcpS, showing Sfp has a much greater labeling efficiency then AcpS, even labeling some other degradation products. Right, Commassie stain of gel. Sfp accounts for the larger band 2nd from the top in the left lane, while AcpS is the darker band near the bottom in the right lane.

Sfp Shows No Difference in Activity for Ybbr Tag or S6 Tag

The available constructs of NMDA-Y1 and the PSD95 protein with the S6 tag (PSD95-S6) were tested with Sfp to determine the labeling efficiency. NMDA–Y1 and PSD95-S6 were tagged with fluorescein-CoA according to the protocol. The samples were

then run on SDS-page and imaged under UV. Comparing the NMDA-Y1 lane to the PSD95-S6 lane, the gel showed Sfp yields high fluorescence with both the Y1 and S6 tag, with no discernable difference in efficiency between the two (figure 5). Since, the Y1 showed the ability to function with both Sfp and AcpS with no discernable difference in activity between the S6 tag, the Y1 tag was used for both the NMDA receptor and PSD95 to allow for flexibility in PPTase selection in future experiments.

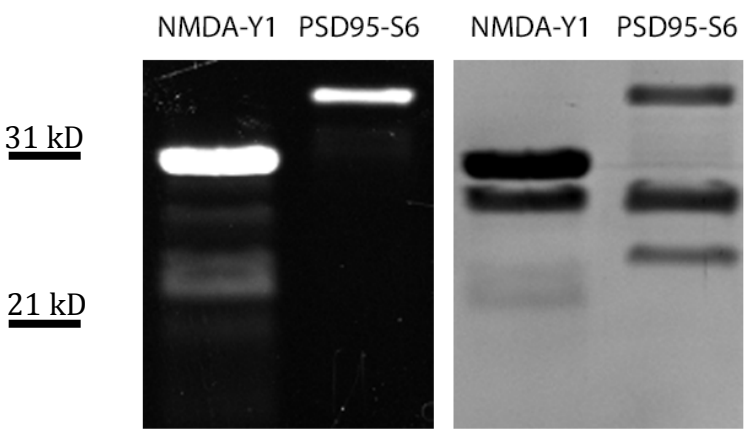

Figure 5 – Comparison of Ybbr tag and S6 tag. Left, fluorescence image of gel. NMDA-Y1 and PSD95-S6 were tagged with fluorescein-CoA. No difference in fluorescence was noted between the Y1 tag and the S6 tag. Right, Commassie Stain of gel, top bands are NMDA and PSD95 of their respective lane. Band right below 31 kD is Sfp.

Testing Palmitoylation ability of PPTases

Development of 2 Assays to Test for Palmitoylation

Previously, the only method used for testing palmitoylation by Ha and coworkers was depositing palmitoylated proteins that had been fluorescently labeled on a lipid bilayer. The bilayer would then be observed with an smTIRF microscope for diffusional movement of fluorescent molecules across the surface. This would show if the protein was tethered to the bilayer, suggesting palmitoylation had occurred. While this method is able to detect if membrane tethering occurred, it gives no indication of palmitoylation efficiency and is time

consuming. Measurement by a microscope can take up to a week to determine if membrane tethering had occurred.

We developed two assays that would allow for the measurement of palmitoylation efficiency within 1-3 days (figure 6). The first assay developed was the "fluorescein chase" assay (figure 6, panels 1, 2a, 2b). The protein is first palmitoylated under normal reaction conditions of 1:5:20 μM PPTase:protein:palmitate-CoA (figure 6, panel 1). This is done either 1 hour at room temperature or overnight at 4° C, until the palmitate-CoA reaction has run to completion. After the reaction has been incubated with palmitate-CoA, fluorescein-CoA is added to the reaction at 20 μM. Any protein with a peptide tag that has not been tagged with palmitate-CoA will then be labeled with fluorescein-CoA (figure 6, panel 2a). The protein can then be separated from the free palmitate-CoA and fluorescein-CoA by SDS-PAGE (figure 6, panel 2b). The fluorescence of the protein can then be measured to determine the efficiency of palmitoylation. The less fluorescence exhibited, the more efficient the palmitoylation labeling.

The second assay developed was the "liposome attachment" assay (figure 6, panels 1, 3a, 3b). The protein is first labeled with a fluorophore, such as Alexa-555. The fluorophore must not be labeling by the PPTase and CoA reaction; we instead use maleimide dyes that attach to free cysteines available in the protein (figure 6, panel 3a). All of our proteins had only 1 available cysteine for fluorophore labeling. After separation of the protein from the free dye and measurement of labeling efficiency, the protein is then palmitoylated using PPTase and palmitate-CoA (figure 6, panel 1). The reaction is once again allowed to go to completion. Small 50 nm liposomes are then extruded according to

(Choi et al. 2012). The palmitoylated proteins are then incubated with 10 mg/mL of the liposomes for 30 minutes at room temperature to allow for membrane tethering (figure 6, panel 3b). The liposomes are then separated from the free unbound protein by a Sepharose CL-4B size exclusion column (GE Healthcare). The fluorescence of the liposome elutions is then measured by fluorimeter to determine the fluorescence intensity associated with the lipids. This thereby estimates how much palmitoylated protein is attached to the liposomes.

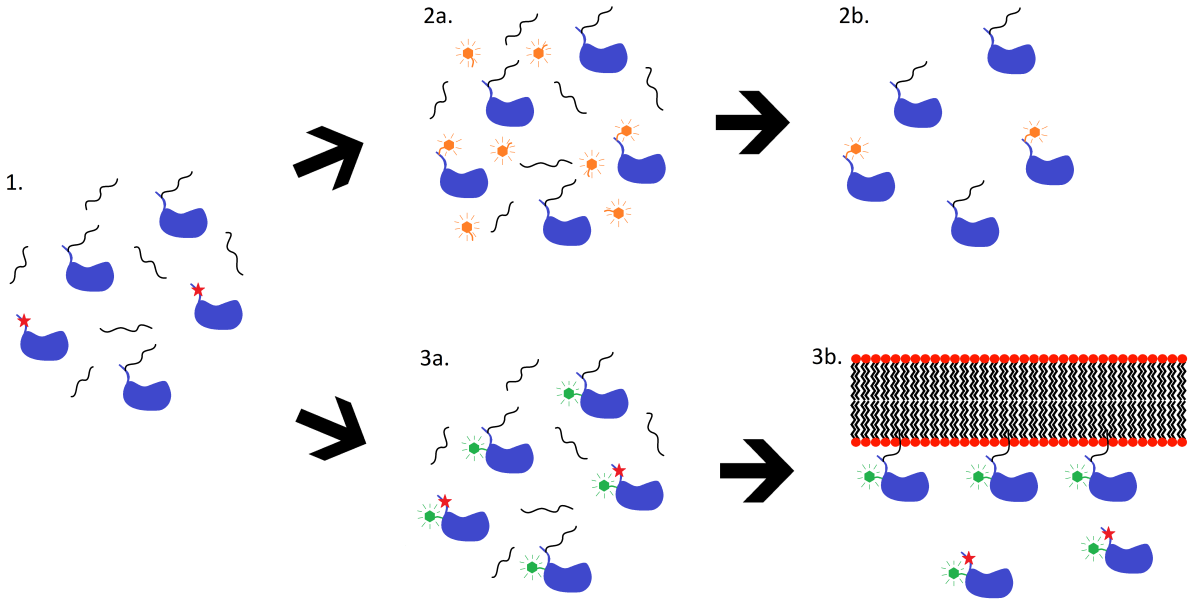

Figure 6 – Assays for determining palmitoylation efficiency. The first method (top steps - 1, 2a, 2b) is the "fluorescein chase" assay. 1. – The protein (blue blob) is first palmitoylated according to the PPTase protocol using palmitate-CoA (black squiggle), this results in most peptide tags (red star) becoming occupied and unable to be tagged again by other CoA derivatives. 2a. - Fluorescein-CoA (orange hexagon) is then added, resulting in any free unlabeled tags, to become labeled with fluorescein. 2b. – All unbound palmitate-CoA and fluorescein-CoA is then removed, allowing for the detection of fluorescein attached to the protein. Lack of fluorescence shows the occurrence of palmitoylation. The second method (bottom steps – 1, 3a, 3b) is the "liposome attachment" assay. 1. – The protein is palmitoylated according to the PPTase protocol using palmitate-CoA. 3a. – The protein is labeled by a fluorophore, via some other means that is not the PPTase reaction (such as a maleimide reaction). Step 1. and 3a. may be done in either order. 3b. – The labeled and palmitoylated protein is incubated with liposomes to allow for membrane tethering. The liposomes with the bound proteins are then separated from the unbound protein by size exclusion chromatography using a CL-4B column. The fluorescence of the liposomes is then measured by a fluorimeter to determine efficiency of palmitoylation.

Sfp Shows No Ability to Palmitoylate Targets with Detergents

Previous work done by Ha and Venkatesh discovered detergents were required for palmitoylate-CoA solubility. Detergents such as 50 mM BOG and 4 mM CHAPS were previously used to aid in the PPTase reaction when palmitate-CoA was used. Sfp was first used due to Sfp displaying greater activity than AcpS (figure 4). When a fluorescein chase experiment of PSD95-Y1 was done with 4 mM CHAPS it was noted that precipitation occurred during the palmitoylation reaction of PSD95-Y1 with Sfp (figure 7). Comparing the sample without and with 4 mM CHAPS (panel A and B of figure 7 respectively), it was noted that the sample with CHAPS precipitated in the presence of the palmitoylation reaction (soluble band, panel B), compared to the sample with no detergent, which did not (soluble band, panel A). It was also found to not occur when the reaction was done without the Mg^{2+} cofactor (-Mg(S) in panel A and B). This led us to the conclusion that palmitoylation was most likely occurring, but the detergent was not enough to keep the palmitoylated PSD95-Y1 from precipitating.

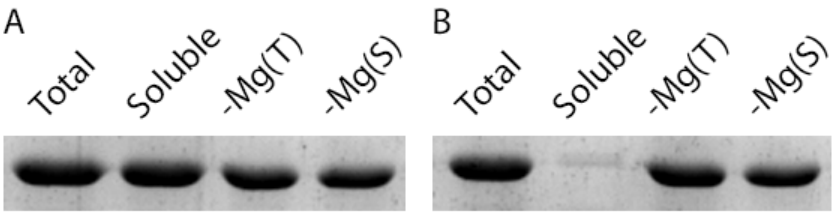

Figure 7 – Palmitoylation of PSD95-Y1 in the presence of CHAPS. Two reactions were done without and with CHAPS (panel A and B respectively): a normal palmitoylate reaction (Total, Soluble), and a negative control [-Mg (T) and –Mg(S)], that lacked the Mg^{2+} cofactor. Total and –Mg (T) indicate how much PSD95-TY1 was originally present in each reaction, before centrifugation. Soluble and –Mg(S) indicate how much PSD95-TY1 protein was left after centrifugation removed any precipitation. Comparison of the Total and Soluble bands for the control and CHAPS shows that CHAPS caused precipitation of the sample. However, if the reaction cannot proceed, then precipitation does not occur, as seen by comparing –Mg(T) and –Mg(S). This suggests that the palmitoylation reaction somehow causes precipitation in the presence of CHAPS.

A report by (Poulio et al. 1995) indicated that ionic detergents, such as CHAPS, were only able to weakly solubilize palmitate for palmitoylation reactions. Instead,

non-ionic detergents such as Tween or Triton proved to be more effective. To compare their effectiveness, 4 mM CHAPS, 0.1% (w/w) Triton X-100, and 0.1% (w/w) Tween 20 were used in the Sfp palmitate reaction with PSD95-Y1. Initial solubility tests showed that Triton X-100 and Tween 20 had no effect on PSD95-Y1 solubility in the palmitate reaction (bottom panels, figure 8). The Triton and Tween samples actually showed larger bands then the low detergent and control bands. This was most likely due to the detergent interactions with the SDS-PAGE gel itself. However, after testing Triton X-100 and Tween 20 for palmitate activity utilizing the fluorescein chase experiment, no decrease in fluorescence between the fluorescein-CoA control (figure 8, panel A) and the fluorescein chase assay was noted (figure 8, panel B). Thus no palmitoylation was observed (figure 8, top panels).

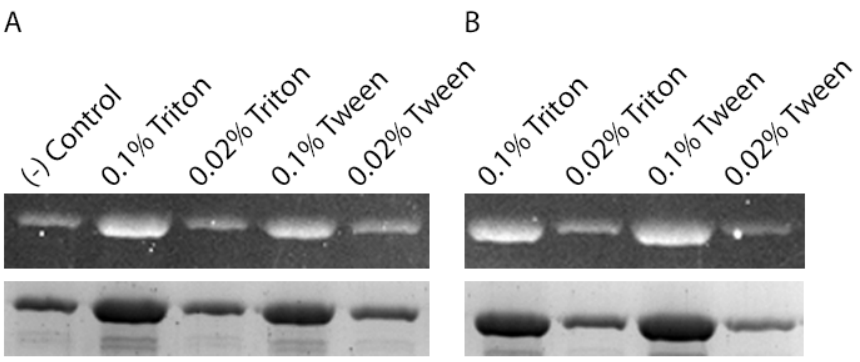

Figure 8 -Testing palmitate activity in the presence of Triton and Tween. Panel A shows the control fluorescein reaction with no palmitate-CoA. The (-) control sample shows the PPTase reaction with no added detergents. 0.1% Triton and 0.1% Tween were used as recommended by (Poulio et al. 1995), as well as 0.02% Triton and 0.01% Tween, which correspond to the CMCs of the detergents. Comparing the positive control to the fluorescein chase samples (panel B), we see no change in fluorescence of the samples, suggesting that no palmitoylation occurred.

We then attempted to detect the palmitoylation of Sfp using the liposome attachment assay. PSD95-Y1 was first labeled by Alexa-555 using a maleimide reaction. Two palmitoylate reactions were done, one in the presence of 0.02% Triton X-100 and the other in 0.01% Tween 20. The reactions were then incubated with 10 mg/mL of 50 nM liposomes. The liposomes were then separated from the free dye by a CL-4B desalting column and the elutions' fluorescence was measured using a fluorimeter. The data revealed

that there was no difference in fluorescence between the control liposomes and the palmitoylated samples in the void volume containing the liposomes, 0-0.6 mL (figure 9). Significant fluorescence was found in the later elutions, showing that fluorescent protein was present, but not bound to the liposomes. This suggested that the protein was unable to tether to the liposomes. Despite high activity with fluorescein-CoA, Sfp showed no activity with palmitate CoA. PPTase specificity for CoA substrate had been previously demonstrated with AcpS, so our results suggest Sfp exhibits a similar ability that results in the selection of fluorescein-CoA but not palmitate-CoA (McAllister et al. 2006).

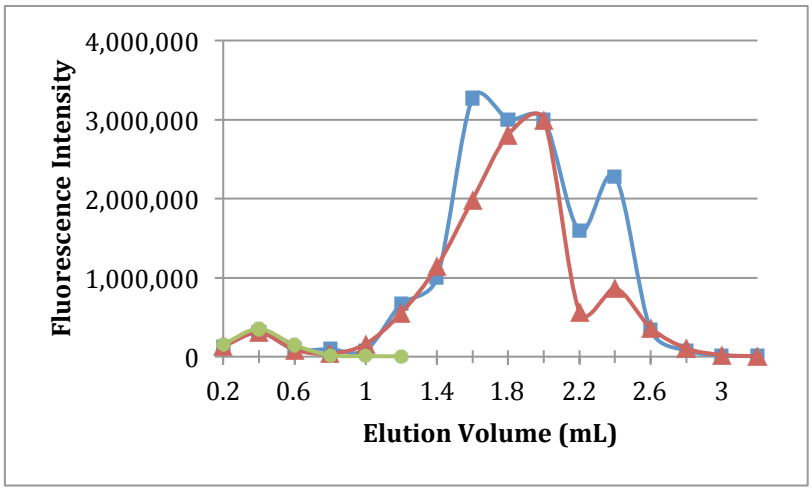

Figure 9 - Fluorescence measurement of liposome attachment assay with Sfp in detergents. Green Circles – Control Liposomes. Blue squares– Elutions of palmitoylation reaction in the presence of 0.02% Triton X-100. Red Triangles – Elutions of palmitoylation reaction in the presence of 0.01% Tween 20. Elution volumes of .2-.6 mL correspond to elutions containing liposomes. Elution volume after .6 mL are elutions containing free unbound protein. Liposomes incubated with palmitoylated protein in the presence of Triton and Tween show no difference in fluorescence compared to control liposomes.

E. coli AcpS Exhibits Palmitoylation with Detergents

We decided to repeat the fluorescein chase assay of PSD95-Y1 in the presence of Triton and Tween with *E. coli* AcpS. *E. coli* AcpS was reported to exhibit low specificity with long chain acyl-CoA derivatives, such as palmitate, and instead prefer short chain acyl-CoA derivatives (McAllister et al. 2006). To compensate for the reported low activity, both reactions of the fluorescein chase assay, first with palmitate-CoA and then fluorescein-CoA, were performed overnight at 4° C. SDS-PAGE analysis showed that the fluorescein chase

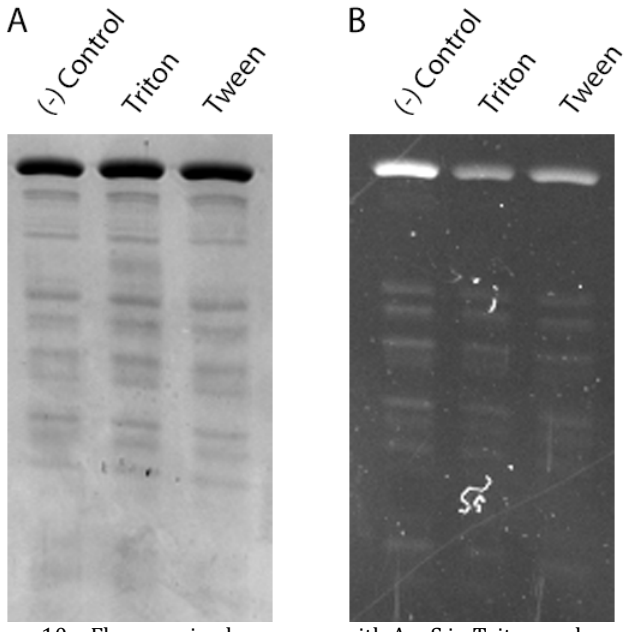

Figure 10 – Fluorescein chase assay with AcpS in Triton and Tween. Left – Commassie stain of gel. Top band is PSD95-Y1, (-) control is a fluorescein-CoA reaction with no palmitate-CoA. Triton is fluorescein chase in the presence of 0.1% Triton X-100. Tween is fluorescein chase in the presence of 0.1% Tween. PSD95-Y1 shows no sign of precipitation in the detergent with palmitoylation reaction. Right – Fluorescence image of gel. Triton and Tween PSD95-Y1 bands show less fluorescence then control fluorescein-CoA band. This shows palmitoylation occurred, preventing the fluorescein-CoA reaction.

reaction with both Triton and Tween exhibited less fluorescence then the control (figure 10, panel B). This implied that palmitoylation had occurred, preventing the labeling of PSD95-Y1 with fluorescein-CoA.

One concern was the high amount of detergent recommended, 0.1% (w/w) Triton or Tween (Poulio et al. 1995). High concentrations of detergents could lead to the solubilization of a lipid bilayer, preventing the single molecule study of these proteins. We ran the same fluorescein chase experiment under 0.02% Triton

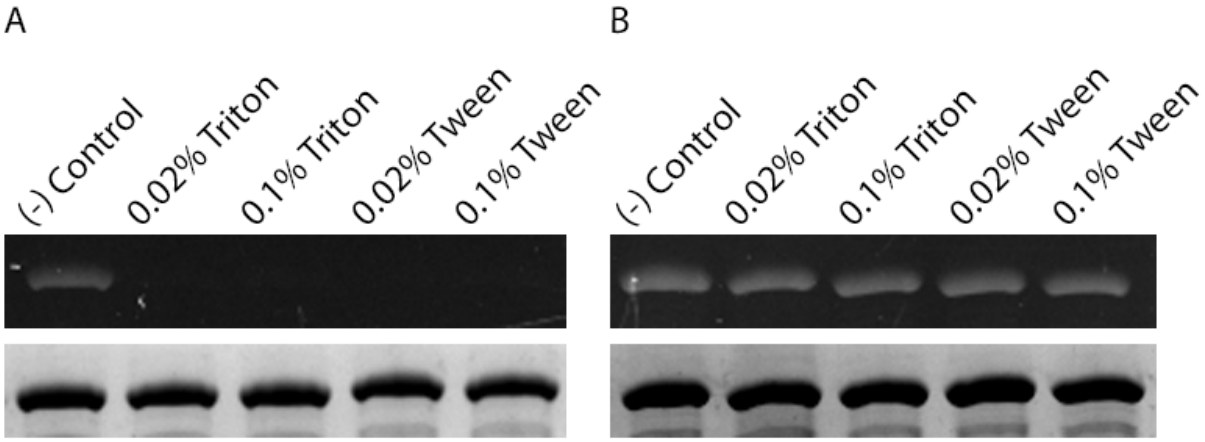

Figure 11 – Determining the effect of Trition and Tween concentration of palmitoylation efficiency. Panel A - UV-image and Commassie Stain of fluorescein chase with palmitate-CoA. Panel B: UV-image and and Commassie Stain of control reaction, with no palmitate-CoA. (-) Control is the reaction with no detergent. Low Triton (L. Tri.) and Low Tween (L. Tw.) are 0.02% Triton and 0.01% Triton respectively. High Triton (H. Tri.) and High Tween (H. Tw.) are 0.1% Triton and Tween. Comparison of the top images shows no fluorescence in the fluorescein chase assay for any concentration of detergents. The large decrease in fluorescence, compared to the fluorescein control, implies palmitoylation was successful.

X-100 and 0.01% Tween 20, close to the CMC of each detergent. Comparison of the fluorescein chase with the lowered detergents (figure 11, panel A) to the fluorescein control (figure 11, panel B) showed the lower concentrations were still able to exhibit palmitoylation to block fluorescein-CoA attachment (figure 11, top panels).

The palmitoylation reaction of AcpS was then measured using the liposome attachment assay. Alexa-555 labeled PSD95-Y1 protein was palmitoylated overnight in the presence of 0.02% Triton X-100 and 0.01% Tween 20 and then incubated with liposomes for 10 minutes. After the liposomes were separated from the free protein by size exclusion chromatography, the fluorescence of the elutions was measured. Examination of the liposome containing elutions, 0-0.6 mL, revealed no increase in fluorescence in either reaction compared to control liposomes (figure 12). This revealed that the protein was once again unable to tether to the liposomes. This left us with two possibilities, either palmitoylation was not occurring and the fluorescein chase assay was providing a false positive, or membrane tethering was still not occurring despite palmitoylation of PSD-95-Y1.

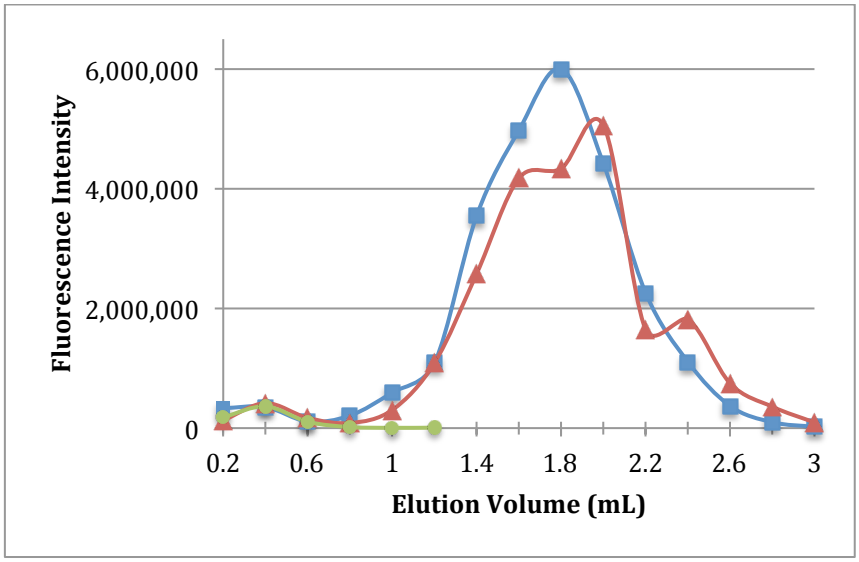

Figure 12 – Fluorescence measurement of liposome attachment assay with AcpS in detergents. Green Circles – Control Liposomes. Blue squares– Elutions of palmitoylation reaction in the presence of 0.02% Triton X-100. Red Triangles – Elutions of palmitoylation reaction in the presence of 0.01% Tween 20. Elution volumes of .2-.6 mL correspond to elutions containing liposomes. Elution volume after .6 mL are elutions containing free unbound protein. Liposomes incubated with palmitoylated protein in the presence of Triton and Tween show no difference in fluorescence compared to control liposomes.

S. pneumoniae AcpS Shows Signs of Palmitoylation but Low Activity

S pneumoniae AcpS was reported to have greater specificity for long chain acyl-CoA derivatives than *E. coli* AcpS (Paulio et al. 2006). An initial purification was done in denaturing conditions with urea, with expectations that *S. pneumoniae* AcpS would require similar conditions as *E. coli* AcpS for solubility. As detailed earlier, four dialyses were attempted (table 5). Samples from the dialyses were then used label PSD95-Y1 with fluorescein-CoA to determine PPTase activity. After the samples were run on an SDS-PAGE gel, very low fluorescence was observed for all detergents (figure 13, panel A).

However, no precipitation was noted for any sample of AcpS (table 5). Since *S. pneumoniae* AcpS had no solubility issues, a native purification of physiological phosphate and NaCl was used to see if it would lead to increases in enzymatic activity. This native sample was then tested using the fluorescein chase assay, as well as a control fluorescein-CoA reaction. The fluorescein assay was used with PSD95-Y1 in the presence of 0.1% Triton. This was run alongside *E. coli* AcpS under the same reaction conditions to compare the two AcpS. A 1-hour sample of *S. pneumoniae* AcpS was also prepared along the overnight samples to determine if time had an effect.

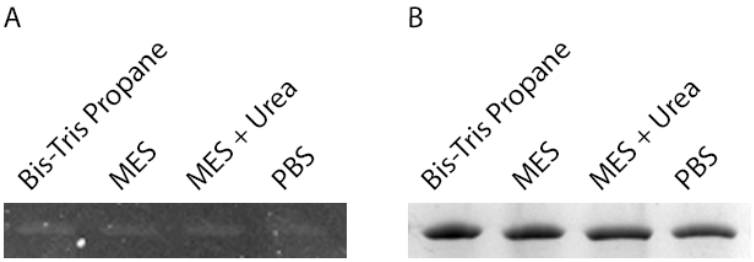

Figure 13 – *S. pneumoniae* AcpS in denatured purification. PSD95-Y1 labeled with fluorescein-CoA utilizing *S. pneumoniae* AcpS after dialysis with different buffers. (Table 5) provides list of dialysis buffers for each lane. Left- Fluorescence image of gel. All lanes show low fluorescence, showing low labeling efficiency of fluorescein-CoA with the AcpS. Right – Commassie stainng of gel.

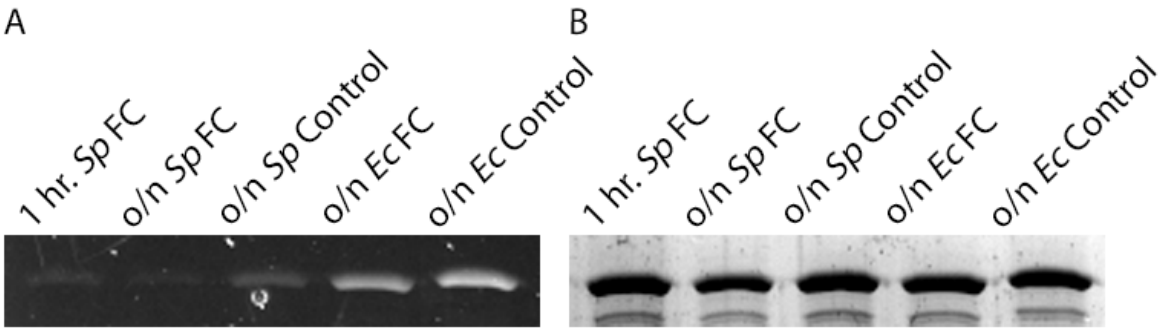

Figure 14 - Fluorescein chase AcpS comparison of PSD95-Y1. "1 hr. *Sp* FC" is the 1 hour fluorescein chase assay with *S. pneumoniae* AcpS. "o/n hr. *Sp* FC" is the overnight fluorescein chase assay with *S. pneumoniae* AcpS. "o/n hr. *Sp* Control" is the overnight fluorescein-CoA control reaction with *S. pneumoniae* AcpS. "o/n hr. *Ec* FC" is the fluorescein chase assay with *E. coli* AcpS. " o/n *Ec* control" is the overnight fluorescein-CoA control reaction with *E. coli* AcpS. Left- fluorescence image of gel. Comparison of controls shows *S. pneumoniae* AcpS exhibits less activity with fluorescein-CoA then *E. coli* AcpS. The fluorescein chase assays both for both AcpS show less fluorescence then their control, suggesting palmitoylation. The 1-hr. *S. pneumoniae* shows more fluorescence then the overnight, suggesting *S. pneumoniae* also needs additional time for the completion of the reaction. Right – Commassie stain of gel, shows bands exhibited the same concentration of PSD95-Y1.

Fluorescence imaging of the SDS-PAGE gel showed that the overnight fluorescein-CoA control of the *S. pneumoniae* AcpS had less fluorescence than the *E. coli* AcpS control (figure 14, panel A). This could be explained by two reasons. First, *S. pneumoniae* AcpS could have less specificity for the Y1 tag, and thus have low activity. Second, S. pnuemoniae AcpS simply exhibits less activity with fluorescein-CoA than *E. coli* AcpS. Comparison of the 1-hour and overnight fluorescein chase assay of *S. pneumoniae* AcpS showed that fluorescein activity still decreased compared to the control (figure 14, panel A). This suggested that palmitoylation was still occurring, despite the low activity with fluorescein-CoA making fluorescence difficult to use as a reporter. However, the 1-hour sample did exhibit more fluorescence than the overnight, meaning *S. pneumoniae* AcpS still requires overnight to completely palmitoylate PSD95-Y1.

S. pneumoniae AcpS was then used to tether PSD95-Y1 to liposomes. PSD95-Y1 was reacted with palmitate-CoA in the presence of 0.02% Triton X-100 overnight at 4° C.

Liposomes were then added to the reaction at a concentration of 10 mg/mL. After separation by a CL-4B size exlusion column, the elutions were measured for fluorescence.

The fluorescence of the liposome containing elutions for the palmitoylated PSD95-Y1 again showed no difference from the control liposomes (figure 15). This led us to the conclusion that *S. pneumoniae* AcpS also resulting in no membrane targeting of PSD95-Y1.

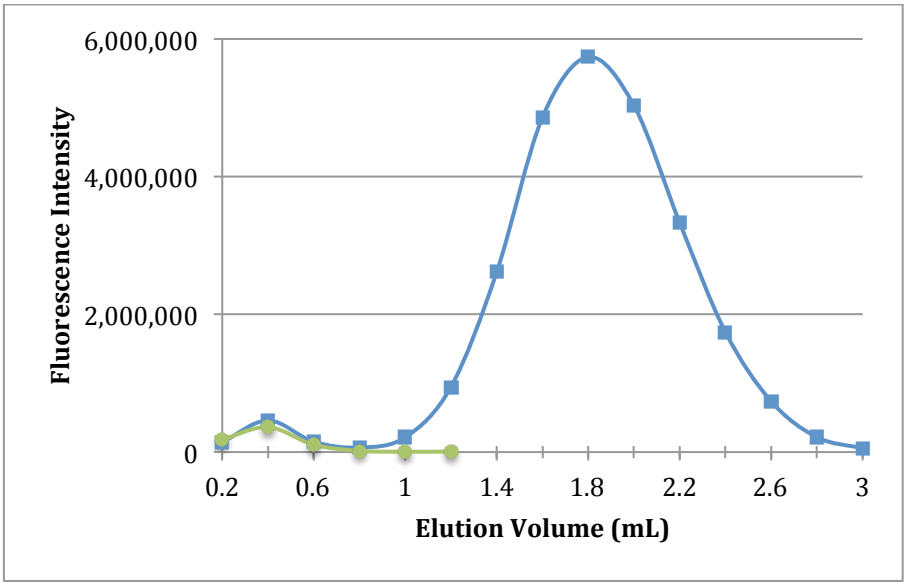

Figure 15 – Liposome binding utilizing *S. pneumoniae* AcpS. Green circles – Control liposomes. Blue Squares – Elutions of overnight palmitoylation reaction with *S. pneumoniae* AcpS in the presence of 0.02% Triton X-100.

Both AcpS results give similar results: the fluorescein chase assay showed signs of palmitoylation, but the liposome attachment assay shows no sign of successful membrane tethering. However, the absence of membrane tethering does not necessarily guarantee that palmitoylation had no occurred. Thus, after analysis of the fluorescein chase assay and the liposome attachment assay together, we can conclude that the PSD95-Y1 is most likely being palmitoylated, but membrane tethering is not occurring.

Discussion

Selection of PPTase Tag sequence

PPTase tag peptide sequences have demonstrated a surprisingly large effect on protein solubility. The addition of the A1 tag to the NMDAR C-terminus tail proved intolerable, despite the careful selection of pH, NaCl levels and detergents (figure 3). While the S6 proved more reliable, with successful protein being purified, it is limited to recognition only by the *B. subtilis* Sfp PPTase. With no results suggesting palmitoylation utilizing Sfp, we cannot use Sfp and the S6 tag (figure 8 and 9). The Y1 tag proved the most tolerated tag by the NMDAR and PSD95 of the tags that were studied. It also functions with both E coli. AcpS and *B. subtilis* Sfp. This allows for the ability to the flexability to use different PPTases in future experiments. However, the selectivity of *S. pneumoniae* AcpS with the Y1 tag is uncharacterized. The possible low specificity of *S. pneumoniae* AcpS for the Y1 tag could be the cause of the low activity in (figure 14 panel A). If *S. pneumoniae* AcpS is utilized for palmitoylation in the future, further work should be done to determine if Y1 is the ideal tag for labeling with *S. pneumoniae* AcpS.

Selection of AcpS for Palmitoylating proteins

Two PPTases were tested, Sfp and AcpS. Only AcpS exhibited palmitoylation activity. Two isoforms of AcpS were tested, *E. coli* AcpS and *S. pneumoniae* AcpS. *E. coli* AcpS clearly demonstrated greater activity than *S. pneumoniae* AcpS with fluorescein-CoA. However, it is difficult to determine which has a higher activity with palmitate-CoA. While both exhibited signs of palmitoylation using the fluorescein chase assay, SDS-PAGE did not reveal if one

exhibits more palmitoylation activity then the other. The low activity of *S. pneumoniae* Acps with fluorescein also makes comparison difficult. While both AcpS are shown to be viable for use in palmitoylation, further quantification of the palmitoylation efficiency between the two AcpS should be done in order to determine the more effective PPTase for palmitoylation. While SDS-PAGE provides a good qualitative assessment, the ability to clearly measure tag efficiency would provide a clear indication of AcpS performance.

With the characterization and success of the palmitoylation reaction, this opens the pathway for many studies on the effect of palmitoylation on the NMDAR and PSD95. One possible study would be to investigate the effects of palmitoylation on the binding kinetics between the NMDAR C-terminal tail and PSD95. The membrane tethering of PSD95 may confer unexpected changes in NMDAR binding, whether by changes in binding kinetics or structural changes.

Palmitoylation Detection using the Fluorescein Chase Assay

The fluorescein chase assay proved able to detect the palmitoylation of PSD95-Y1 with both forms of AcpS. A decrease in fluorescence was noted for both palmitoylation reactions using AcpS, showing that the extent of the labeling reaction with palmitate-CoA could be measured by the decrease in labeling of fluorescein-CoA (figure 11 and figure 14). However several limitations were noted after viewing the SDS-PAGE gels and comparison the liposome attachment assay. First, the method is limited by the activity of the PPTase with fluorescein-CoA. If fluorescein-CoA is unable to be attached to the protein by the PPTase, it would not be possible to observe a change in fluorescence. This proved an issue with *S. pneumoniae* AcpS. With a low baseline fluorescein-CoA activity, determination of the

efficiency of palmitoylation by AcpS proved difficult. Both *E. coli* AcpS and *B. subtilis* Sfp have already exhibited specificity for various CoA derivatives, as shown in this experiment and (McAllister et al. 2006).

A large limitation of the fluorescein chase assay was the precarious solubility of palmitate-CoA and palmitoylated proteins. This made filtration and concentration difficult without causing the loss of sample or the disruption of the palmitoylation reaction. This meant we could not detect labeling efficiency of fluorescein-CoA using absorbance spectroscopy. Often the palmitoylated proteins would bind to filters used in spin filtration columns, concentrators, and columns resulting in an inaccurate labeling efficiency as only the protein labeled with fluorescein and not palmitate was retained.

Another possible issue is that the assay does not detect the type of CoA substrate being attached to the protein. This brings up the possibility of false positives occurring. The attachment of other CoA substrates to the protein would still result in the prevention of fluorescein-CoA attachment, leading to impression that palmitoylation is occurring even though it is not. While palmitate-CoA is the most likely substrate being attached, quality assessment of the palmitate-CoA purity would be required to rule out this uncertainty. This probability is exacerbated by the preference of *E. coli* AcpS for short acyl chains; meaning possible damaged palmitate-CoA would be preferred over the full-length palmitate-CoA.

Membrane Tethering Detection Using Liposome Attachment Assay

The liposome attachment assay displayed conclusive results but the cause of these results were left open to many possible interpretations. The liposome attachment assay

clearly showed that the product from the reaction with the protein, PSD95-Y1 and palmitate-CoA, was unable to tether to lipid membranes, despite evidence of palmitoylation by AcpS using the fluorescein chase assay. However, the cause behind this inability is unclear. The most likely case is that the single addition of a palmitate moiety is insufficient for membrane tethering of PSD95-Y1. This would give us the result seen, where the fluorescein chase assay reports the successful palmitoylation of the protein, but no protein is seen on the liposomes. Other posttranslational lipid modifications, such as myristate and farnesyl attachment have been shown to only provide modest to weak affinity for the membrane (Peitzsch et al. 1993 and Silviu et al. 1994). The weak membrane targeting means that the protein is easily detached from the membrane. Instead, a protein generally requires the attachment of two lipid chains to confer a strong enough affinity to remain attached to the membrane (Resh et al. 2006). PSD95 has also been shown to require the palmitoylation of both cysteines on the N-terminus for proper sorting to the synapse (El-Husseini et al. 2000). A dually palmitoylated PSD95 should be tested to determine if this is the cause. Alternatively, the liposome attachment assay could be used to test a protein that is known to only require one palmitoylation modification for membrane tethering.

A second issue is the presence of detergents during the palmitoylation reaction. While detergents are required for palmitoylation to occur, the detergent could interfere with the affinity between the palmitate and the membrane. The detergent adds nonpolar properties to the solution, and provides a surrounding similar to the liposomes. While this results in increased solubility for the palmitate, this could result in a decrease in the binding constant of the protein and the lipid membrane. This would result in the protein not attaching to the liposome but instead staying in the favorable detergent environment. If

the detergent is too strong, it could also completely solubilize the lipid bilayer, destroying any membrane. A buffer exchange might be required to cause the binding of the palmitated protein on the membrane. However, care must be used during the buffer exchange to prevent the precipitation of the palmitoylated protein with the loss of the detergent.

Evaluation of Palmitoylation Assays

While both assays have limitations, the assays proved to be invaluable in quantifying and characterizing palmitoylation with PPTases. The results of the fluorescein chase assay with AcpS led to the conclusion that PPTase activity was occurring with palmitate-CoA. Meanwhile the results of the liposome attachment assay showed that membrane tethering was not occurring. This shows that the assays are best used in conjunction with each other to alleviate their limitations. A liposome attachment assay can only tell us if membrane tethering has occurred, it does not indicate that palmitoylation was necessarily unsuccessful. It only can guarantee the positive result: if membrane tethering did occur, then palmitoylation occurred. A fluorescein chase assay allows us to determine the situation where membrane tethering did not occur. It could be the case that palmitoylation did not occur. It could also be the case that palmitoylation did occur but was insufficient for membrane tethering, as seen in this case. Each assay alone would have been unable to arrive at this conclusion. The combination of these assays removes the uncertainty our previous experiments experienced on the efficiency and effect of the palmitoylation reaction.

Future Works

While some questions remain in order to completely verify the results of both assays, we feel confident that palmitoylation utilizing the PPTase reaction was a success. This opens up possible future studies on the effect of palmitoylation on NMDAR and PSD95. One avenue of study would be the use of single molecule Förster resonance energy transfer (smFRET) to observe the binding kinetics of the palmitoylated proteins. smFRET takes advantage of energy transfer that occurs between two fluorescent probes that are in close proximity to one another. The efficiency of this energy transfer is proportional to the distance between the two probes. This would allow the reporting of binding events between PSD95 and the NMDAR, while also providing the distance between locations on PSD95 and the NMDAR. Alternatively, by selecting two sites of study on a single protein, the intramolecular distance between the two can be determined. This would allow us to study structural and conformational changes caused by palmitoylation on PSD95 or the NMDAR.

Bibliography

Berg JM, Tymoczko JL, Stryer L. (2002). Chapter 15, Signal-Transduction Pathways: An Introduction to Information Metabolism. Biochemistry. 5th edition. New York: W H Freeman.

Berg, O. G., & von Hippel, P. H. (1985). Diffusion-controlled macromolecular interactions. Annu Rev Biophys Biophys Chem, 14, 131-160. doi:10.1146/annurev.bb.14.060185.001023

Bhattacharya, S., Chen, L., Broach, J. R., & Powers, S. (1995). Ras membrane targeting is essential for glucose signaling but not for viability in yeast. Proceedings of the National Academy of Sciences of the United States of America, 92(7), 2984-2988.

Chi, C. N., Bach A Fau - Gottschalk, M., Gottschalk M Fau - Kristensen, A. S., Kristensen As Fau - Stromgaard, K., Stromgaard K Fau - Jemth, P., & Jemth, P. Deciphering the kinetic binding mechanism of dimeric ligands using a potent plasma-stable dimeric inhibitor of postsynaptic density protein-95 as an example. (1083-351X (Electronic)). doi:D - NLM: PMC2934690 EDAT- 2010/06/26 06:00 MHDA- 2010/10/06 06:00 CRDT- 2010/06/26 06:00 AID - M110.124040 [pii] AID - 10.1074/jbc.M110.124040 [doi] PST - ppublish

Choi, U. B., Weninger, K. R., & Bowen, M. E. (2012). Immobilization of proteins for single-molecule fluorescence resonance energy transfer measurements of conformation and dynamics. Methods Mol Biol, 896, 3-20. doi:10.1007/978-1-4614-3704-8_1

Constantinides, P. P., & Steim, J. M. (1986). Solubility of palmitoyl-coenzyme A in acyltransferase assay buffers containing magnesium ions. Arch Biochem Biophys, 250(1), 267-270.

El-Husseini, A. E., Craven, S. E., Chetkovich, D. M., Firestein, B. L., Schnell, E., Aoki, C., & Bredt, D. S. (2000). Dual palmitoylation of PSD-95 mediates its vesiculotubular sorting, postsynaptic targeting, and ion channel clustering. J Cell Biol, 148(1), 159-172.

El-Husseini, A. E.-D., Schnell, E., Dakoji, S., Sweeney, N., Zhou, Q., Prange, O., . . . Bredt, D. S. Synaptic Strength Regulated by Palmitate Cycling on PSD-95. Cell, 108(6), 849-863. doi:10.1016/S0092-8674(02)00683-9

Feng, W., & Zhang, M. (2009). Organization and dynamics of PDZ-domain-related supramodules in the postsynaptic density. Nat Rev Neurosci, 10(2), 87-99. doi:10.1038/nrn2540

Folch, J., & Lees, M. (1951). Proteolipides, a new type of tissue lipoproteins; their isolation from brain. J Biol Chem, 191(2), 807-817.

Fukata Y Fau - Bredt, D. S., Bredt Ds Fau - Fukata, M., & Fukata, M. Protein Palmitoylation by DHHC Protein Family BTI - The Dynamic Synapse: Molecular Methods in Ionotropic Receptor Biology.

Hayashi, T., Thomas, G. M., & Huganir, R. L. (2009). Dual palmitoylation of NR2 subunits regulates NMDA receptor trafficking. Neuron, 64(2), 213-226. doi:10.1016/j.neuron.2009.08.017

Ho, G. P., Selvakumar, B., Mukai, J., Hester, L. D., Wang, Y., Gogos, J. A., & Snyder, S. H. (2011). S-nitrosylation and S-palmitoylation reciprocally regulate synaptic targeting of PSD-95. Neuron, 71(1), 131-141. doi:10.1016/j.neuron.2011.05.033
Johnsson, K., & George, N. (2010). Methods for protein labeling based on acyl carrier protein: Google Patents.
Lambalot, R. H., Gehring, A. M., Flugel, R. S., Zuber, P., LaCelle, M., Marahiel, M. A., . . . Walsh, C. T. A new enzyme superfamily — the phosphopantetheinyl transferases. Chemistry & Biology, 3(11), 923-936. doi:10.1016/S1074-5521(96)90181-7
McAllister, K. A., Peery, R. B., & Zhao, G. (2006). Acyl carrier protein synthases from gram-negative, gram-positive, and atypical bacterial species: Biochemical and structural properties and physiological implications. J Bacteriol, 188(13), 4737-4748. doi:10.1128/jb.01917-05
Munro, J. B., Gorman, J., Ma, X., Zhou, Z., Arthos, J., Burton, D. R., . . . Mothes, W. (2014). Conformational dynamics of single HIV-1 envelope trimers on the surface of native virions. Science, 346(6210), 759.
Neff, R. A., 3rd, Gomez-Varela, D., Fernandes, C. C., & Berg, D. K. (2009). Postsynaptic scaffolds for nicotinic receptors on neurons. Acta Pharmacol Sin, 30(6), 694-701. doi:10.1038/aps.2009.52
Paoletti, P., Bellone, C., & Zhou, Q. (2013). NMDA receptor subunit diversity: impact on receptor properties, synaptic plasticity and disease. Nat Rev Neurosci, 14(6), 383-400. doi:10.1038/nrn3504
Peitzsch, R. M., & McLaughlin, S. (1993). Binding of acylated peptides and fatty acids to phospholipid vesicles: Pertinence to myristoylated proteins. Biochemistry, 32(39), 10436-10443. doi:10.1021/bi00090a020
Poulio, J. F., & Beliveau, R. (1995). Palmitoylation of brain capillary proteins. Int J Biochem Cell Biol, 27(11), 1133-1144.
Resh, M. D. (2006). Trafficking and signaling by fatty-acylated and prenylated proteins. Nat Chem Biol, 2(11), 584-590.
Roth, A. F., Feng, Y., Chen, L., & Davis, N. G. (2002). The yeast DHHC cysteine-rich domain protein Akr1p is a palmitoyl transferase. J Cell Biol, 159(1), 23-28. doi:10.1083/jcb.200206120
Scannevin, R. H., & Huganir, R. L. (2000). Postsynaptic organization and regulation of excitatory synapses. Nat Rev Neurosci, 1(2), 133-141. doi:10.1038/35039075
Sheng, M. (2001). The postsynaptic NMDA-receptor--PSD-95 signaling complex in excitatory synapses of the brain. J Cell Sci, 114(Pt 7), 1251.
Silvius, J. R., & l'Heureux, F. (1994). Fluorometric Evaluation of the Affinities of Isoprenylated Peptides for Lipid Bilayers. Biochemistry, 33(10), 3014-3022. doi:10.1021/bi00176a034
Sunbul, M., Zhang, K., & Yin, J. (2009). Chapter 10 using phosphopantetheinyl transferases for enzyme posttranslational activation, site specific protein labeling and identification of natural product biosynthetic gene clusters from bacterial genomes. Methods Enzymol, 458, 255-275. doi:10.1016/s0076-6879(09)04810-1
Xue, L., Gollapalli Dr Fau - Maiti, P., Maiti P Fau - Jahng, W. J., Jahng Wj Fau - Rando, R. R., & Rando, R. R. A palmitoylation switch mechanism in the regulation of the visual cycle. (0092-8674 (Print)).

Yin, J., Lin, A. J., Golan, D. E., & Walsh, C. T. (2006). Site-specific protein labeling by Sfp phosphopantetheinyl transferase. Nat Protoc, 1(1), 280-285. doi:10.1038/nprot.2006.43

Zhang, J., Lewis, Steven M., Kuhlman, B., & Lee, Andrew L. Supertertiary Structure of the MAGUK Core from PSD-95. Structure, 21(3), 402-413. doi:10.1016/j.str.2012.12.014

Zhou, Z., Cironi, P., Lin, A. J., Xu, Y., Hrvatin, S., Golan, D. E., . . . Yin, J. (2007). Genetically encoded short peptide tags for orthogonal protein labeling by Sfp and AcpS phosphopantetheinyl transferases. ACS Chem Biol, 2(5), 337-346. doi:10.1021/cb700054k